Seismic Observations using Ocean Bottom Seismometers around Kuchierabujima Volcano

Hiroshi Yakiwara[1], Shuichiro Hirano[1], Yusuke Yamashita[2], Hiroshi Shimizu[3], Kazunari Uchida[3], Kodo Umakoshi[4], Kazuo Nakahigashi[5,6], Hiroki Miyamachi[1], Mitsuharu Yagi[7], Hisao Kanehara[7] and Shigeru Nakao[1]

[1] Graduate School of Science and Engineering, Kagoshima University
[2] Disaster Prevention Research Institute, Kyoto University
[3] Graduate School of Science, Kyushu University
[4] Graduate School of Fisheries and Environmental Studies, Nagasaki University
[5] Graduate School of Science, Kobe University
[6] Now, School of Marine Resources and Environment, Tokyo University of Marine Science and Technology
[7] Faculty of Fisheries, Nagasaki University

Abstract

The remarkable eruption on Kuchierabujima, which occurred on May 29, 2015, had the potential to disrupt land seismic observation if the volcanic activities had expanded. Since relatively deep-volcano-tectonic (DVT) earthquakes under the volcano may have extended into the sea region around the island, we deployed four ocean bottom seismometers (OBSs) on the seafloor at distances at approximately 6.5 km from the crater. During the OBS observation period from July 3 to October 9, 2015, 303 volcanic earthquakes were detected. The daily numbers and the temporal amplitude changes indicate that seismic activities declined in the middle of August. However, only nine of the events were DVT earthquakes, and we were unable to identify any clear differences between the hypocenter distribution characteristics of the DVT events discussed in previous studies and those of our observations. However, since the temporal tendency of daily earthquake numbers derived from our OBS data resembled that compiled by the Japan Meteorological Agency using real-time land data, when eruption expansions occur on a small-scale remote island such as Kuchierabujima, OBS observations can provide a useful backup to efforts aimed at grasping the seismicity.

1. INTRODUCTION

Kuchierabujima is one of the most active volcanoes along the Kyushu-Ryukyu arc of southwestern Japan (Fig. 1). Based on tephra stratigraphy, Geshi and Kobayashi (2006) constructed a volcanological history of Kuchierabujima volcanic activities covering the last 30,000 years. In their study, they identified two major pumice and scoria eruptions between 1,500 and 1,100 years ago, the formation of a volcanic edifice, lava flow emissions, and repetitive Vulcanian-type eruptions and phreatomagmatic explosions over the last 10,000 years. Historical eruptions of the volcano since 1841 have been Vulcanian-type eruptions and phreatic explosions (Geshi and Kobayashi, 2006).

The Sakurajima Volcano Research Center, Disaster Prevention Research Institute (DPRI) of Kyoto University has conducted continuous seismic observations of the volcano since December 1991 (e.g., Triastuty et al., 2009). Additionally, the Geological Survey of Japan, which is operated by the National

H.YAKIWARA, S.HIRANO, Y.YAMASHITA, H.SHIMIZU, K.UCHIDA, K.UMAKOSHI,
K.NAKAHIGASHI, H,MIYAMACHI, M.YAGI, H.KANEHARA, S.NAKAO

Institute of Advanced Industrial Science and Technology (AIST), has performed ground deformation observations using Global Positioning System (GPS) data in cooperation with DPRI since 2004 (Saito and Iguchi, 2006).
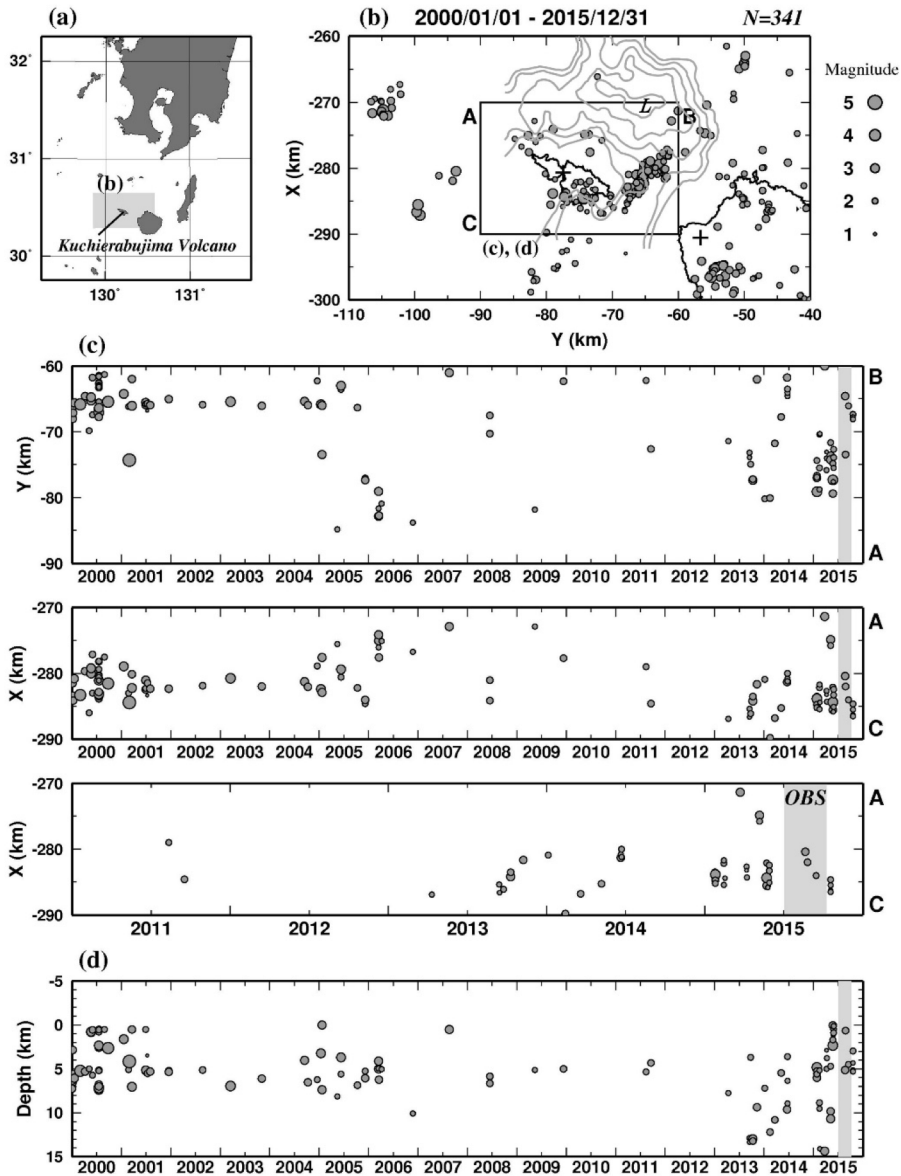
Fig. 1: Medium- and long-term seismicity of crustal earthquakes around the volcano. (a) Overview of volcano location. (b) Epicenter distribution of crustal earthquakes over the last 16 years. The Nansei-Toko Observatory for Earthquakes and Volcanoes (NOEV), Kagoshima University, identified these earthquakes using data derived from regional real-time seismic stations. The gray curves are isograms of residual gravity anomalies (after Iguchi et al., 2007). "L" indicates a low-residual gravity anomaly. (c) Earthquake spatiotemporal distribution. (d) Time-depth relationship of these earthquakes. The epicenters of (b) and (c) are plotted on a plane rectangular coordinate system of Japan.

Before the August 3, 2014 eruption, four clear ground deformations accompanied by an obvious increase of shallow earthquakes were observed in the volcano (Geological Survey of Japan and Sakurajima Volcano Research Center, 2016). Triastuty et al. (2009) studied the activities of shallow volcano tectonic (SVT) earthquakes close to Mt. Shindake crater and concluded that the SVT earthquake seismicity resulted from tensional stress accumulation caused by the intrusion of hydrothermal fluid.

However, few studies have been carried out on the hypocenter distribution and seismicity of volcano tectonic (VT) earthquakes occurring at deeper levels under and around the volcano, even though Tameguri and Iguchi (2007) reported on the isolated occurrence of relatively deep volcano-tectonic (DVT) earthquakes with depths of several kilometers, and Iguchi (2007) reported that DVT earthquakes had occurred off the northeastern coast of the island in 1996 and 1999. That study concluded that the hypocenters of these DVT earthquakes were located in the vicinity of the eastern and southern rim of a low-gravity anomaly region (Komazawa et al., 2007) where a caldera structure was presumed to exist (Fig. 1(b)). However, there are few available details about the seismicity of DVT earthquakes because such earthquakes have been rare in recent years.

On May 29, 2015, a remarkable eruption took place at the crater of Mt. Shindake, which is the active crater of the volcano. Pyroclastic flow and surge descended from the eruption plume, and reached the western coast of the island. In response, the Japan Meteorological Agency (JMA) issued a Volcanic Alert Level 5: 'Evacuate' and local residents and sojourners were required to depart from the island within the day. This evacuation proved troublesome for all island infrastructure requiring electric power, including the observation systems for volcanic activity and their related wireless communication networks, which use electricity provided by the island's heavy oil power generation plant.

If the expansion of eruption activities had forced a halt to the delivery of heavy oil supplies to the island, ground-based seismic monitoring and geodetic observations would have been forced to cease operations as well. DVT earthquakes had been occasionally observed in areas under, adjacent, and outside the volcano since 2000 (Fig. 1), and the expansion of volcanic activity could mean an increase in DVT earthquakes in regions adjacent to the volcano.

If we were restricted to data collected from land seismic stations, it would be impossible to detect small DVT earthquakes in the adjacent regions, and thus impossible to precisely determine the hypocenters of such earthquakes. With these points in mind, we decided to perform seismic observation at the seafloor surrounding the volcano using ocean bottom seismometers (OBSs).

There have been no interruptions to the oil supply because volcanic activities gradually subsided following the June 19, 2015 eruption, and the volcano has been quiescent since then, so the evacuation order was called off on December 25, 2015. Although only a few DVT earthquakes (the observation of which is our primary objective) were recorded, we were able to observe the process by which seismic activity declined. Thus, in this paper, we report on the results of analyses conducted using seismic data collected from our OBSs in conjunction with JMA land station data.

2. OBSERVATIONS AND DATA

As a part of the No. 417 educational cruise of the training ship Nagasaki Maru (842 gross tons) operated by the Faculty of Fisheries of Nagasaki University, we deployed four pop-up-type OBSs onto the seafloor around Kuchierabujima on July 3, 2015, 35 days after the May 29, 2015 eruption. These OBSs were released via free-fall mode. Figure 2 shows the distribution of the seismic stations used in this investigation. The OBSs were deployed on the seafloor at a horizontal distance of approximately 3.5 nautical miles (6.5 km) from Mt. Shindake crater because of a JMA warning that the area within a 2.0 nautical mile (3.7 km) radius of the crater may have been enlarged by volcanic activity expansion. The water depths of these OBS stations were from 480 to 610 meters. The possibility of submarine eruptions declines if there is a certain amount of water depth.

Later, we used another multipurpose vessel, the No. 3 Aoi Maru (4.9 gross tons, Nagata Port, Yakushima Island) to determine the positions of the OBSs on the seafloor via an acoustic survey. Throughout

the voyages, the positions of both the Nagasaki Maru and No. 3 Aoi Maru were logged each second using differential GPS (DGPS) systems. The positions of the OBSs on the seafloor were determined using both acoustic distance measurements and the vessel's DGPS position data. As the vessel was not equipped with onboard navigation systems, our DGPS compass and a personal computer, in which electric navigation charts (ENCs) issued by the Japan Coast Guard had been installed, were set up on the vessel during the cruises. By plotting the vessel's position superimposed on the ENCs, we carefully guided the boat vessel to the objective points. We successfully retrieved all OBSs via pop-up mode on October 30, 2015 using the No. 3 Aoi Maru. However, in order to conserve battery power and to prevent physical damage to the OBS sensors, we had timed the recording to end prior to their retrievals. As a result, the number of observational days was about 98, from July 3 through October 9.
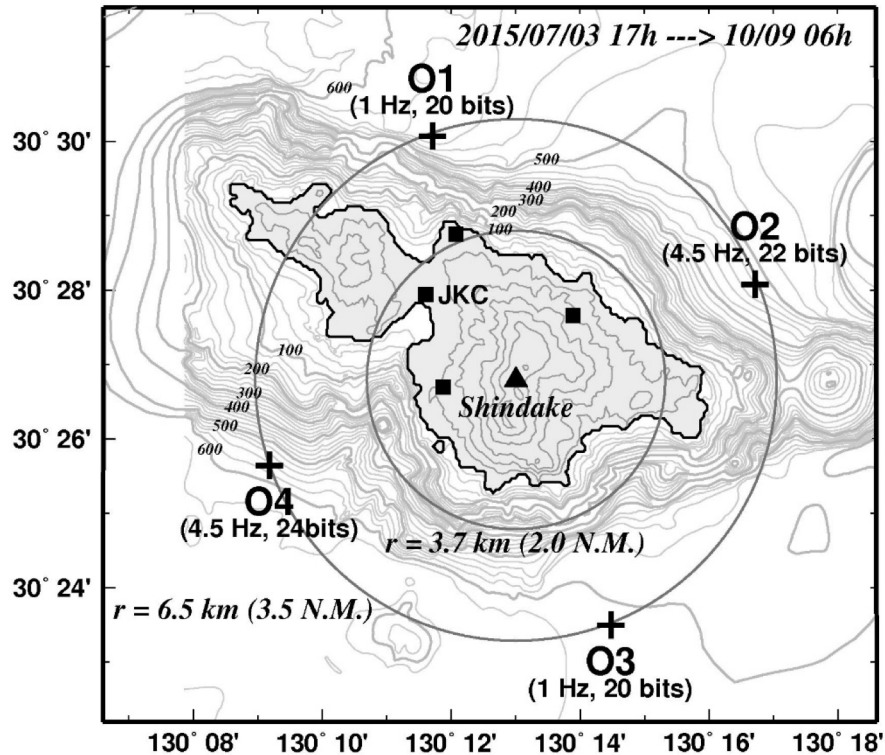

Fig. 2: Distribution of seismic stations in this investigation. Crosses indicate the positions of ocean bottom seismometers (OBSs) on the seafloor. Solid squares show the land seismic stations operated by the JMA. The solid triangle shows Mt. Shindake crater. The contour line and thick isobath intervals are set at 100 meters while thin isobaths are depicted every 20 meters. The inner and outer circle radii are 3.7 km and 6.5 km (2.0 and 3.5 nautical miles), respectively.

These OBSs were equipped with a three-component velocity sensor consisting of a digitizer, a digital recorder, and an accurate internal clock with very small drift rate (0.02–0.05 s/day). The natural frequencies of velocity sensors were 1 Hz (Station O1 and O3) or 4.5 Hz (Station O2 and O4). The analog/digital (A/D) resolutions were set to 20 bits for Stations O1 and O3, 22 bits for Station O2, and O3 and 24 bits for Station O4. The sampling frequency of all OBSs was set to 200 Hz. Since the internal clock of an OBS cannot be corrected during the seafloor deployment because radio waves cannot be transmitted through the water, we measured the time differences between the OBS clocks and a GPS timing module on the vessels just before deployment and immediately after retrieval. Assuming constant drift rates for each OBS, we were able to

correct the OBS clock values throughout the observation period. These time calibrations were successful for all OBSs.

The continuous waveform data obtained by the OBSs were then merged with the continuous waveform data collected by four JMA land stations (Fig. 2), after which we plotted the merged continuous waveform on paper charts in order to visually identify the volcanic earthquakes. Using the three-component seismic waveform of the selected earthquakes, we then read out the arrival times of P- and S-waves at each seismic station in order to determine hypocenter locations and magnitudes. However, it was difficult for the OBSs to determine the hypocenters of very shallow micro-earthquakes close to Mt. Shindake crater with sufficient accuracy because seismic waves attenuate along the propagation path, and because the high noise levels present on the seafloor are larger than the weakened waveforms.

3. OBSERVED VOLCANIC EARTHQUAKES DURING THE OBS OBSERVATION PERIOD

The spatiotemporal distribution of regional crustal earthquakes that occurred during the period from 2000 to 2015 is shown in Fig. 1. The hypocenters were selected from a catalog of the Nansei-Toko Observatory for Earthquakes and Volcanoes (NOEV, Kagoshima University), which meant that our OBS observation period was included in the spatiotemporal distributions (Fig. 1). It should be noted that our OBSs observations were carried out during a period when seismic activity was relatively low.
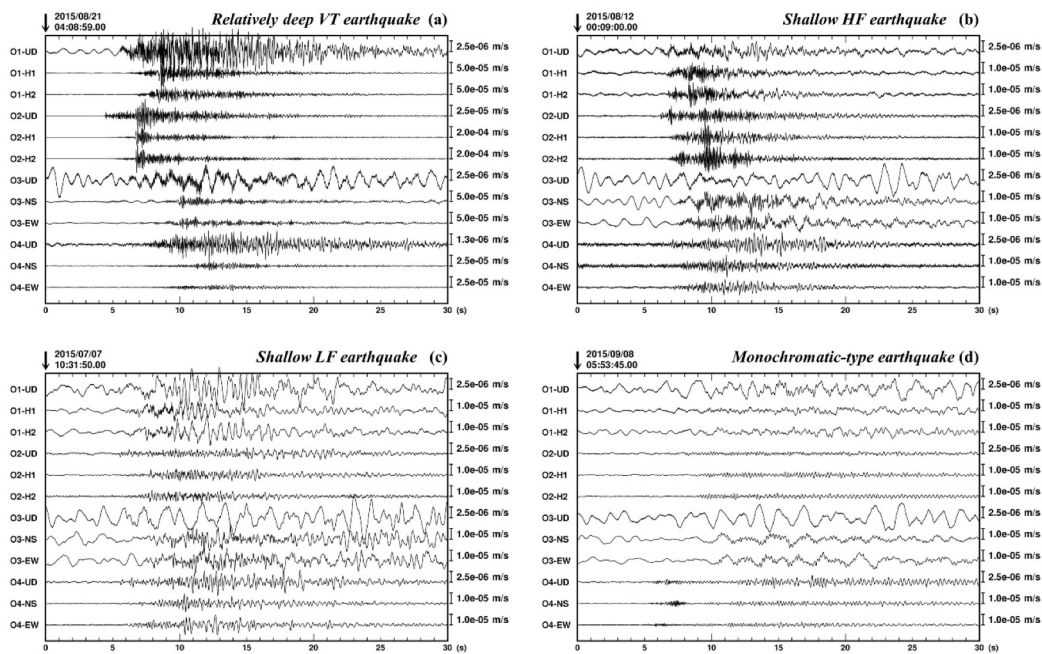

Fig. 3: Waveform examples for each earthquake type observed via OBS. The three component waveforms of all OBSs are shown. UD refers to the vertical component waveform. H1 and H2 are the two horizontal components. (a) Relatively deep volcano-tectonic (DVT) earthquakes. (b) Shallow high-frequency (SHF) earthquakes. (c) Shallow low-frequency (SLF) earthquakes. (d) Monochromatic-type (MT) earthquakes.

Based on the specifications of Triastuty et al. (2009), Fig. 3 shows examples of four volcanic

earthquake waveforms recorded by each OBS: DVT earthquakes, shallow high-frequency (SHF) earthquakes, shallow low-frequency (SLF) earthquakes, and monochromatic-type (MT) earthquakes. SHF earthquakes have a wide frequency range spectra of 6 to 25 Hz, while SLF earthquakes are dominated by lower frequencies of around 1 to 5 Hz (Triastuty et al., 2007). With the exception of the DVT earthquake, these volcanic events occurred at very shallow depths within several hundred meters around Mt. Shindake crater (Triastuty et al., 2009). Of these volcanic earthquakes, only the DVT earthquake observations obtained using OBSs were effective for improving the accuracy of our hypocenter determination process.

In Fig. 3, the initial motions of the observed waveforms are conspicuously attenuated at Station O3, which led us to conclude that, unluckily, the OBS had landed on a thick unconsolidated seafloor deposit. Furthermore, the 1 Hz sensor stations (O1 and O3) tended to record long-period waveforms generated by ocean waves. The predominant DVT earthquake frequencies were from several to 10 Hz, which are obviously high in comparison with those generated by ocean waves. Thus, using the above factors, we calculated the amplitudes of each waveform by averaging the maximum vertical component amplitudes of the two OBSs equipped with 4.5 Hz sensors (Stations O2 and O4). Ultimately, 303 events whose seismic amplitudes were larger than or equal to 5.0×10^{-7} m/s were identified during the OBS observation period.
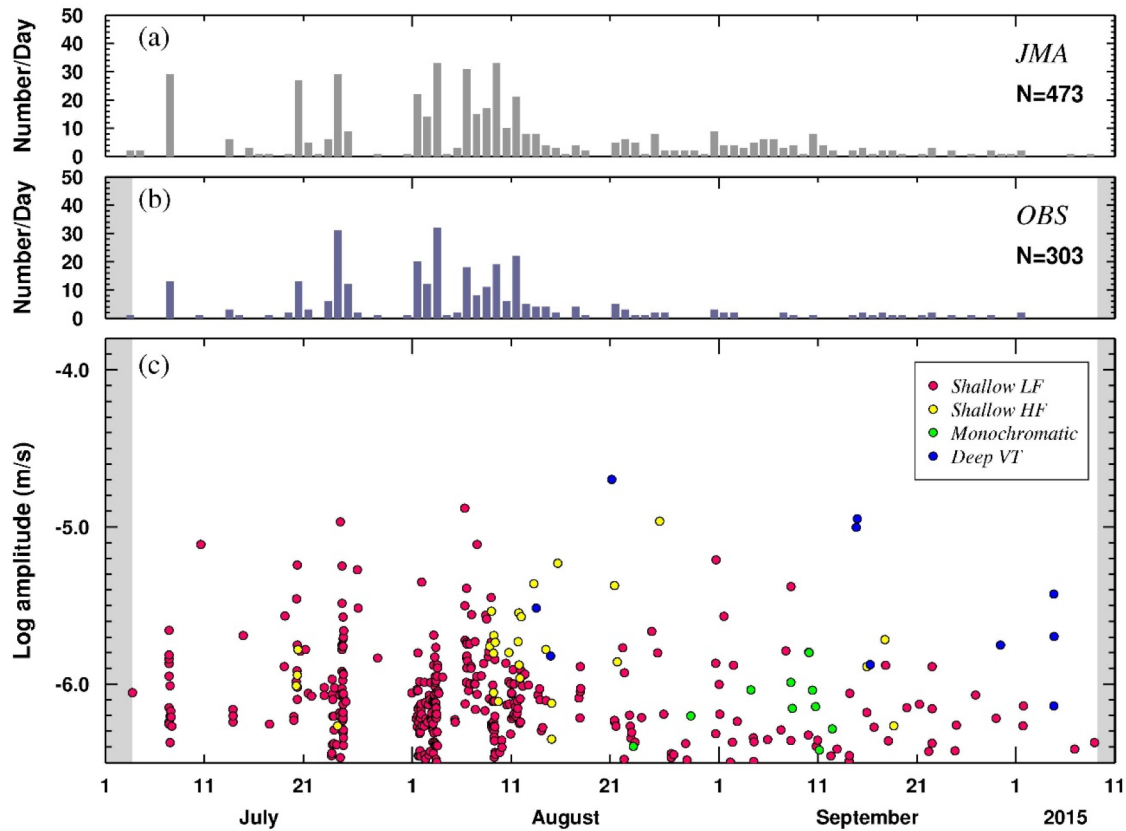

Fig. 4:   Daily numbers and time changes of observed volcanic earthquake amplitudes. (a) Daily numbers of volcanic earthquakes (Details of Volcanic Activity, JMA). (b) Daily numbers of earthquakes that could be identified by maximum amplitude data collected at OBS Station O2 and O4. (c) Amplitude time changes of earthquakes shown in (b). The colors show the earthquake types.

Figure 4(b) shows daily numbers of the observed volcanic earthquakes. In Fig. 4(c), the observed amplitude of each earthquake was plotted against the time axis. This figure clearly shows that the daily numbers of volcanic earthquakes decreased in the middle of August. The SLF earthquakes were prominent

and clustered before the middle of August, while the SHF earthquakes increased during the first half of that month. No clear cluster of SLF earthquakes was observed after the middle of August. Additionally, only a few SHF earthquakes occurred after the end of August and the amplitudes of these above-mentioned earthquake types showed a general tendency to decrease over time after the end of August. Meanwhile, MT earthquakes showed isolated occurrences during the period from the end of August to the middle of September when SLF and SHF earthquake activities declined. Collectively, the volcanic earthquake activity decline took place in the middle of August 2015.

4. HYPOCENTER DISTRIBUTION OBTAINED BY OBS

4.1. Seismic velocity model and estimation of station corrections

In general, P- and S-wave arrival times at an OBS are significantly later than would be expected based on velocity model calculations, primarily owing to thick unconsolidated sediments beneath the seafloor. Consequently, observed travel times from hypocenters to the seismic stations are much longer than the calculated theoretical travel times. Since these time delays significantly influence the locus obtained via hypocenter determination calculations, the estimation of correction values, called station correction, which take the P- and S-arrival delay times into consideration, is very important. The models shown in Fig. 5(a) were derived from the results of other observations, which combined OBSs with land seismic stations, performed in and around the Tokara and Nansei-Syoto Islands since 2014 (Yakiwara et al., personal comm.). The P- and S-wave arrival time station corrections for each station were estimated as follows:
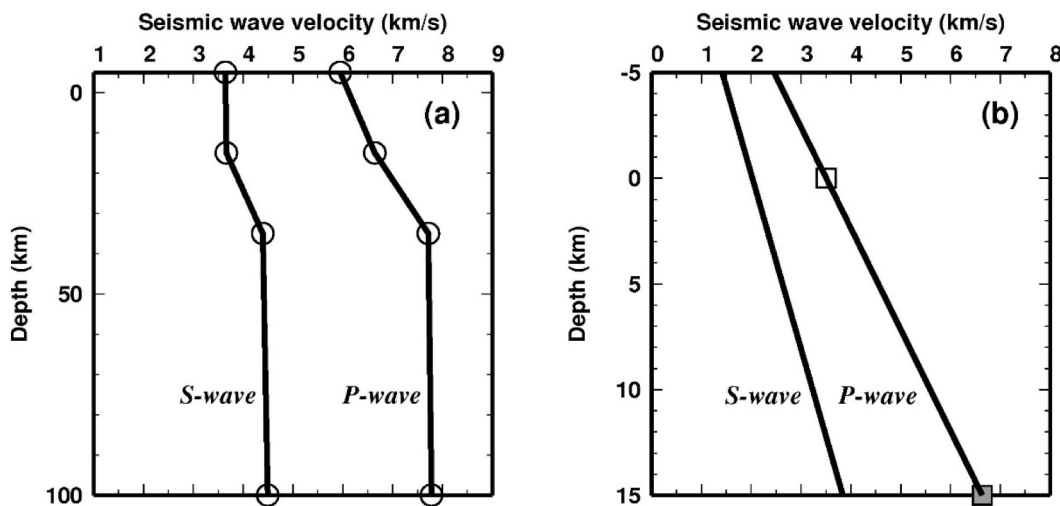

Fig. 5: One-dimensional (1D) P- and S-wave velocity models used in this investigation. (a) Regional P- and S-velocity models. These models were derived from regional data obtained by island seismic stations and OBSs observations in and around the Tokara Islands (Yakiwara et al., 2015, personal comm.). Open circle velocities were estimated by inversion schemes. The velocities between the circles were obtained by linear interpolation. (b) Local P- and S-velocity models used to locate the volcanic earthquakes in and around Kuchierabujima. The P-wave velocity at a depth of 15 km (gray square) is identical to that of (a). An open square (3.50 km/s) at a depth of 0 km was determined using a grid searching method. Assuming $V_p/V_s = 1.73$ (constant ratio), we assigned the S velocities. The velocity gradient above a depth of 0 km equals that between a depth of 0 and 15 km.

H.YAKIWARA, S.HIRANO, Y.YAMASHITA, H.SHIMIZU, K.UCHIDA, K.UMAKOSHI,
K.NAKAHIGASHI, H,MIYAMACHI, M.YAGI, H.KANEHARA, S.NAKAO

(1)　　　　We selected 27 regional earthquakes that occurred around the Tokara Islands within the OBS observation period.

(2)　　　　Assuming the hypocenter locations were correct, we calculated travel time residuals of the P- and S-wave arrivals at each station by using the P- and S-wave velocity model shown in Fig. 5(a).

(3)　　　　We then subtracted the value of P-wave travel-time residuals at Station JKC (Fig. 2) from the values of each other station. The travel time residuals were adjusted so that the P-wave travel time residuals at Station JKC became 0.00 s.

(4)　　　　In order to estimate station corrections, the obtained relative travel-time residuals were then averaged for each station.

Because in comparison with the distance from Kuchierabujima to the regional earthquakes hypocenters around the Tokara Islands seismic stations were located in a sufficiently narrow area, the velocity difference between the one-dimensional (1D) model and the true velocity resulted in seismic wave delays that were nearly identical. Based on this consideration, we decided to accept the adjusted values of 4) above as the station corrections.

Figure 6 shows the station corrections of P- and S-waves of each station. A positive value for the station correction (red circle) indicates a seismic wave arrival delay. As for the OBSs, the station corrections show large positive values that are caused by sediment deposits beneath the seafloor. The largest correction (estimated at Station O3) is consistent with conspicuous seismic wave attenuations. Contrastingly, the estimated corrections of the land seismic station were small.
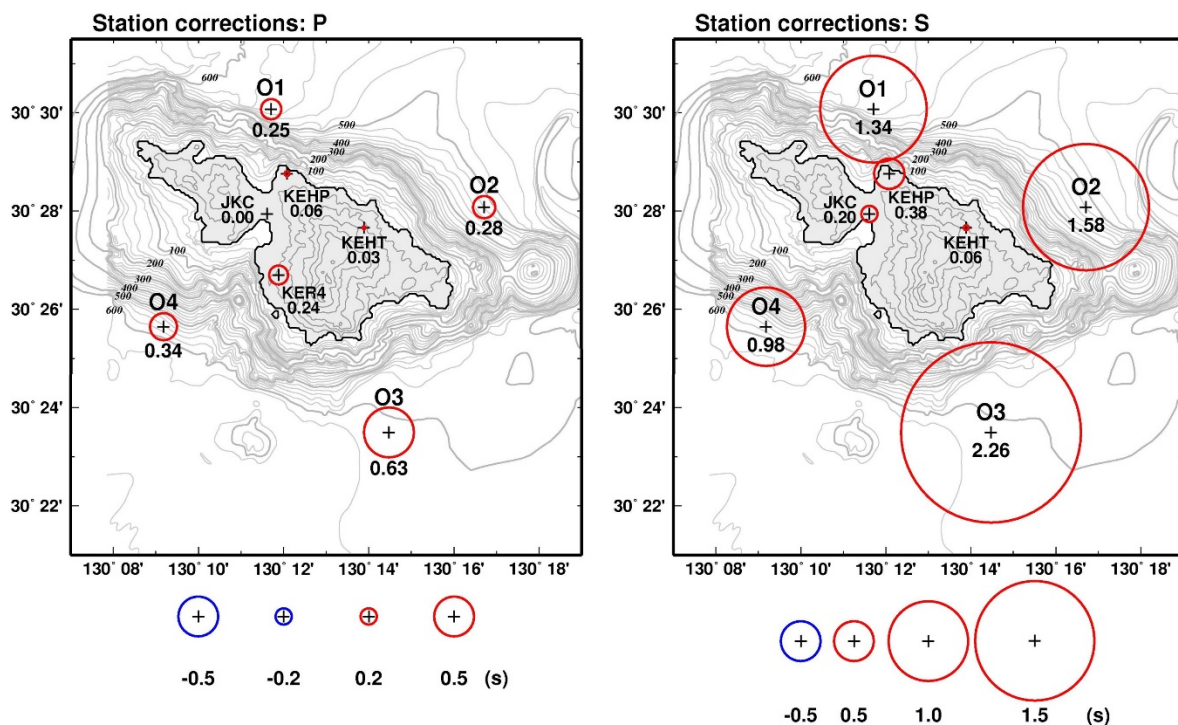

Fig. 6: Station corrections at each OBS and land seismic station used in this investigation. Positive and negative values (red and blue circles) show the delay and advance, respectively, relative to P arrivals at Station JKC. In general, remarkably large and positive values were estimated on S arrivals at the OBSs due to unconsolidated sediment deposits beneath the seafloor. Note, a correction of S arrivals at Station KER4 was not obtained in this analysis because no horizontal component data was available.

4.2. Hypocenter distribution during the OBS observation

Seismic velocity models are also required when using P- and S-wave arrival times to determine the hypocenters of seismic events. Because the regional velocity models shown in Fig. 5(a) were too fast to be applied to the shallow depth range of volcanic regions, we reconstructed the 1D P- and S-wave velocity models shown in Fig. 5(b) as follows:

(1)　　　　The P-wave velocity at a depth of 15 km was identical to that of Fig. 5(a).

(2)　　　　The P-wave velocity (3.50 km/s) at a depth of 0 km was determined by a grid searching method in which we iteratively performed hypocenter determinations by changing the velocity from 2.0 to 4.0 km/s by 0.1 km/s.

(3)　　　　Assuming Vp/Vs = 1.73 (constant ratio), we assigned the S velocities.

(4)　　　　The velocity gradient above a depth of 0 km was assumed to equal that between depths of 0 and 15 km.

For the 67 earthquakes observed during our observation period, we identified P- and S-wave arrival times at each station using seismic waveforms displayed on computer monitors. Using the identified P- and S-arrivals and velocity models of Fig. 5(b), we then determined the hypocenter locations of the volcanic events. Of these earthquakes, 62 volcanic earthquakes were located in and around Kuchierabujima Volcano, and were plotted in Fig. 7.
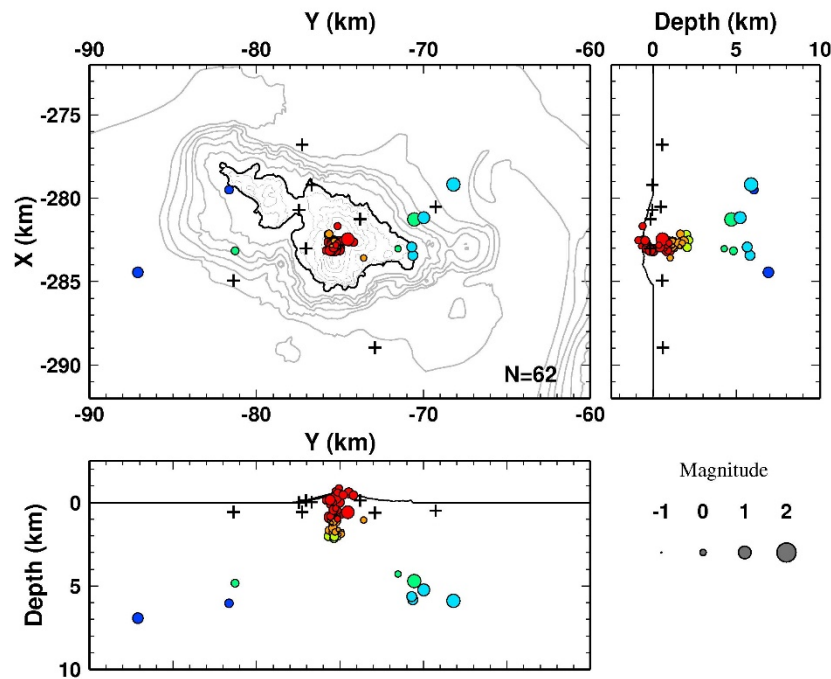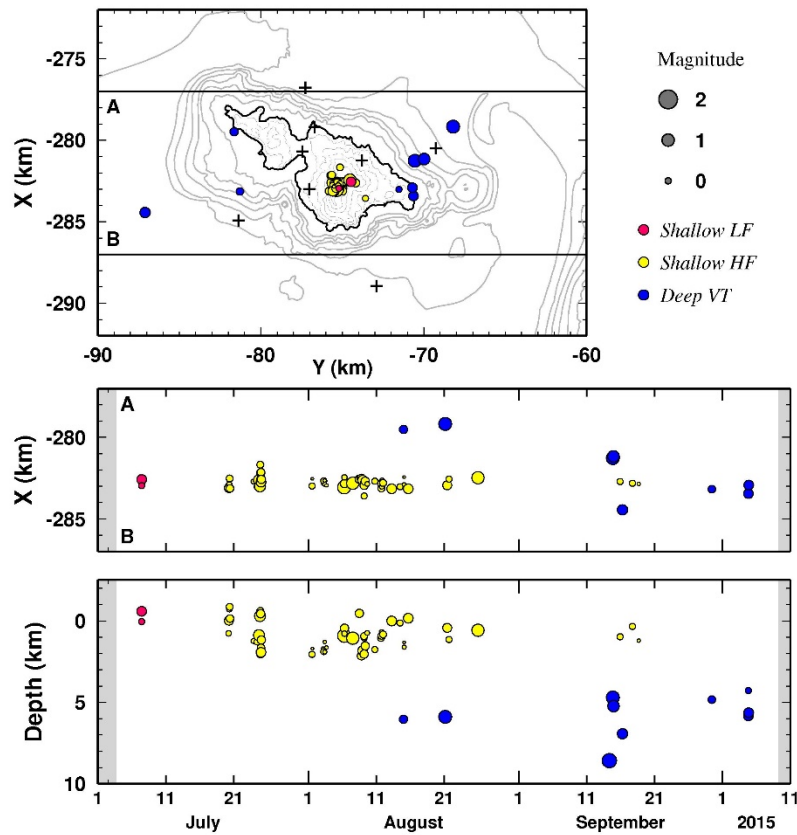

Fig. 7: Hypocenter distribution during the OBS observation period. The circle colors correspond to the hypocenter depths.

However, only nine earthquakes recorded during the OBSs observation period matched our targeted DVT earthquake type, and the magnitudes of these DVT earthquakes were 1.1 or less. The depth range of these DVT earthquakes was from 4.7 km to 6.9 km, and no DVT earthquake was located deeper than 7 km during the observation period. Of these DVT earthquakes, three were micro-earthquakes that occurred beneath the east end of the island, were nearest to Mt. Shindake crater, and had magnitudes between 0.0 and 0.6. Three other DVT earthquakes had magnitudes between 0.9 and 1.1, and were located off the northeast shore of the island. The final three DVT earthquakes were observed on the west side of the island. One had a magnitude of 0.3 and was located beneath the west end of the island at a depth of about 6 km, while the final two earthquakes, whose magnitudes were 0.2 and 0.7, occurred off the west coast of the island. Thus, in terms of DVT earthquakes, the area in and around the volcano was mostly calm.

H.YAKIWARA, S.HIRANO, Y.YAMASHITA, H.SHIMIZU, K.UCHIDA, K.UMAKOSHI,
K.NAKAHIGASHI, H,MIYAMACHI, M.YAGI, H.KANEHARA, S.NAKAO

In contrast, the remaining 53 earthquakes were SHF and SLF events that occurred in the area close to Mt. Shindake crater. The depth range of these events was from the Earth's surface to a depth of 2.1 km. A seismicity gap from 2.1 km to 4.7 km in depth was plotted between the relatively deep earthquakes and shallow events close to the crater, even though very few DVT earthquakes were observed. However, the uncertainties related to identifying seismic wave arrival times at each station might have resulted in the vertically elongated hypocenter area for the SHF and SLF earthquakes. Additionally, the increased OBS data uncertainty might have arisen from the longer epicenter distances, and from the high sea bottom noises in comparison with those of land seismic stations.

Figure 8 shows the spatiotemporal distributions of the 62 hypocenters used in this analysis. As the figure shows, the SHF earthquakes were dominant until the middle of August 2015. Conversely, no DVT earthquakes occurred in the vicinity of the volcano until the beginning of August (Fig. 4). After the middle of August, the numbers of SHF earthquake hypocenters obviously decreased because the numbers of the events decreased, and because few relatively large amplitude events occurred (Fig. 4). Three DVT earthquakes were identified around the volcano in the middle of August, while the remaining DVT earthquakes were identified after the middle of September. As for the SLF earthquakes, only three events

were identified because the initial phases of the other events were too weak to precisely read out the arrival times.

Fig. 8:   Spatiotemporal distributions of the volcanic earthquakes during the OBS observation period. The circle colors show earthquake types.

5. DISCUSSION

Because temporal changes of hypocenters and focal mechanisms of VT earthquake are closely related to stress changes, the dearth of DVT earthquakes during our observation period implies that clear stress state changes caused by the charge or discharge of magma did not occur in the deep portion, e.g., main magma reservoir, of the volcano. In 2010 and 2011, the JMA began global navigation satellite system (GNSS) observations at four stations on the volcano's flank in order to facilitate monitoring of volcano crustal deformations. Other GNSS stations operated by the National Research Institute for Earth Science and Disaster Resilience (NIED), AIST, and the Geospatial Information Authority of Japan (GSI) were also installed on the volcano. Because of the eruption disasters that occurred in 2014 and 2015, among the baselines between GNSS stations on the volcano, we could only identify one temporal baseline length change (JMA station) and no clear baseline length changes were recorded during our OBS observation period (Fukuoka Volcanic Observation and Information Center and Kagoshima Meteorological Observatory, 2016), which is consistent with the scarcity of DVT earthquakes throughout the period. As for the volcano's main reservoir, Yamamoto et al. (2017) performed repeated precise leveling surveys in order to estimate pressure sources. Assuming that the pressure source was located under Mt. Shindake crater, they estimated the source depth of 7.0 km. However, no DVT earthquakes occurred in the region neighboring the main pressure source.

The DVT earthquake hypocenter regions determined during our observation period have also been recognized in previous studies covering periods when no eruptions were observed. Iguchi (2007) mentioned the active regions of DVT earthquakes off the northeast coast of the island, which occurred in 1996 and 1999. The hypocenters of these events were located on the east and south rim of a caldera, which was estimated based on low-gravity anomalies (Iguchi, 2007; Komazawa et al., 2007). As the DVT earthquake hypocenters observed in the present investigation were also located close to the southern rim of the low-gravity anomaly region, thereby implying the existence of a caldera structure, DVT earthquakes could be expected to occur under the present geological structure in the same manner as those occurring during the 1996 and 1999 activities. In addition, Tameguri and Iguchi (2007) pointed out isolated DVT earthquake occurrences in the volcano's west side region in 2005, which matches our observational results. Collectively, there are no clear seismic activity differences between the results of our observation and these previous study results.

Since there was the possibility that observations on the island could be obstructed by the expansion of eruption activities, we initiated OBS observations shortly after the May 29, 2015 eruption. Figure 4(a) shows the daily numbers of volcanic earthquakes along with other volcanic information contained in the "Details of Volcanic Activity" issued by JMA, including real-time seismic station data on the island. The temporal daily number trends of Fig. 4(a) resemble those of Fig. 4(b), which are derived from our OBS data. Although the OBS data was only available for post-processing (not real-time processing), the temporal change of seismicity related to volcanic activity could also be observed.

If eruption activities continue expanding, all or several stations for ground-based seismic monitoring may stop observations. Figure 9(a) shows the hypocenter locations determined by the use of data collected from just four OBSs. A total of 59 hypocenters were also located from among the 62 earthquakes plotted in Fig. 7. As for the remaining three earthquakes, we could not locate the hypocenters because less than four P-arrivals were available. Although several of the epicenters shown in Fig. 9(a) shifted from 3 to 5 km, almost all of the epicenters were located at nearly the same position when compared with the epicenters plotted in Fig. 7. However, the hypocenter distribution in N-S and E-W cross sections differed considerably from that of Fig. 7. Furthermore, we were unable to estimate the hypocenters for SHF earthquakes with any precision because no S-arrival times were observed for the earthquakes. In other words, only four P-arrival times were available. In the case of the hypocenter determination using only OBSs data, it was difficult to locate the hypocenters with sufficient levels of accuracy. Hence, these results and Fig. 4 suggest that the observations taken using just four OBSs, without ground-based seismic data, could also be useful for grasping epicenter distribution, daily earthquake numbers, and temporal amplitude changes of the volcanic earthquakes.

On the other hand, Fig. 9(b) shows the hypocenter distribution that was determined using data observed at the four OBSs and a land seismic station, JKC. The obtained hypocenter distribution of the 62

earthquakes strongly resembles that of Fig. 7. Thus, the hypocenter determination was clearly improved simply by adding data collected from a land seismic station to the OBSs data. Collectively, seismic observations using OBSs can provide data efficiently at times when several seismic stations have been interrupted by the expansion of eruption activities.

Since the possibility of submarine eruptions declines if there is a certain amount of water depth, and since there is little chance that the OBSs will suffer direct damage due to the eruptions, they can record ground motions continuously related to volcanic activities. Hence, when eruption expansions occur in a small-scale remote island like Kuchierabujima, the observation using OBSs can provide a useful backup to efforts aimed at grasping seismic activities related to the volcanic event.
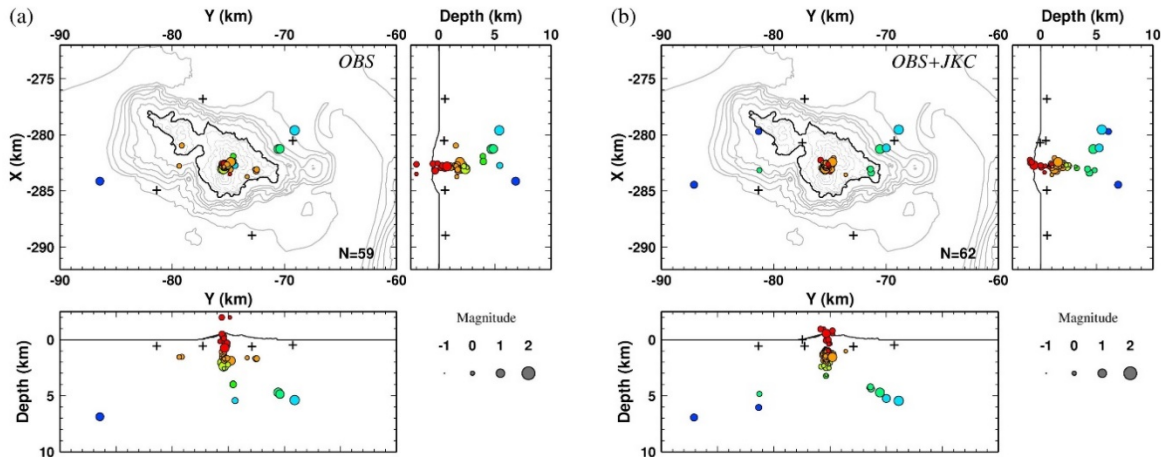

Fig. 9:   Hypocenter distribution in the OBS observation period. (a) Hypocenter distribution determined using only OBSs data. (b) Hypocenter distribution determined using data collected from OBSs and a land seismic station (JKC).

6.   CONCLUSION

In response to the powerful eruption of Kuchierabujima Volcano on May 29, 2015, we deployed four OBSs onto the seafloor around the island on July 3, 2015 and retrieved them on October 30, 2015. Corrections to all the devices' internal clocks were completed successfully. Since the OBS timers were set to stop recording prior to the retrieve, the observation period was from the deployment day to October 9, 2015 (about 98 days). The continuous waveform data obtained by the OBSs were then merged with the continuous waveform data collected by four land stations operated by the JMA.

After determining the maximum amplitude using the waveform data of each recorded earthquake, 303 events were identified during the OBS observation period. The daily numbers and temporal changes of these earthquakes indicate the decline in volcanic earthquake activity took place in the middle of August 2015. After estimating travel time corrections for each station, hypocenter determinations were performed. The results showed that 62 volcanic earthquakes were located in and around the volcano, only nine of which were DVT earthquakes, the primary focus of our observations.

The depth range of these DVT earthquakes was from 4.7 to 6.9 km. Additionally, a seismicity gap from a depth of 2.1 to 4.7 km existed between the DVT earthquakes and shallow events close to the crater. Finally, we were unable to identify any hypocenter distribution characteristic differences in our DVT earthquake observations and those of previous studies.

Although few DVT earthquakes were observed, we were able to examine the process in which seismic activity declined and found that the temporal tendency of daily volcanic events derived from OBS

data closely resembled that obtained by JMA using real-time land seismic station data. Thus, when rapid eruption expansions occur on a small-scale remote island like Kuchierabujima, OBS observations can provide a useful backup to efforts aimed at grasping the seismicity related to volcanic activities, even though pop-up-type OBS data are not available in real-time.

References

Geological survey of Japan, AIST, Sakurajima Volcano Research center, DPRI, Kyoto Univ., 2016. Ground deformation at the summit region in the Kuchierabujima Volcano for ten years before August 3, 2014 eruption. Report of Coordinating Committee for Prediction of Volcanic Eruption, 119, 359-363.

Geshi, N., Kobayashi, T., 2006. Volcanic activities of Kuchinoerabujima Volcano within the last 30,000 years. Bull. Volcanol. Soc. Japan, 51, 1-20.

Fukuoka Volcanic Observation and Information Center, Kagoshima Meteorological Observatory, 2016. Bulletins on Volcanic Activity of Kuchierabujima Volcano (November, 2016). pp. 1-8.

Iguchi, M., 2007. Volcanic activity at Kuchinoerabujima Volcano in 2006. Report of Special Project on Practical Study on Prediction of Phreatic Eruption and Its change at Kuchierabujima Volcano, Japan; Dias. Prev. Res. Inst., Kyoto Univ., Japan, pp. 9-16.

Komazawa, M., Nakamura, K., Yamamoto, K., Iguchi, M., Akamatsu, J., 2007. Gravity anomalies of Kuchierabujima Volcano. Report of Special Project on Practical Study on Prediction of Phreatic Eruption and Its change at Kuchierabujima Volcano, Japan; Dias. Prev. Res. Inst., Kyoto Univ., Japan, pp.49-52.

Saito, E., Iguchi, M., 2006. Ground deformation detection at Kuchinoerabujima Volcano by continuous GPS with sample atmospheric correction. Bull. Volcanol. Soc. Japan, 51, 21-30.

Tameguri, T., Iguchi, M., 2007. Seismic activities around Kuchinoerabujima Volcano. Report of Special Project on Practical Study on Prediction of Phreatic Eruption and Its change at Kuchierabujima Volcano, Japan; Dias. Prev. Res. Inst., Kyoto Univ., Japan, pp. 25-28.

Triastuty, H., Iguchi, M., Tameguri, T., Yamazaki, T., 2007. Hypocenters, spectral analysis and source mechanism of volcanic earthquakes at Kuchinoerabujima: high-frequency, low-frequency and monochromatic events. Report of Special Project on Practical Study on Prediction of Phreatic Eruption and Its change at Kuchierabujima Volcano, Japan; Dias. Prev. Res. Inst., Kyoto Univ., Japan, pp. 17-24.

Triastuty, H., Iguchi, M., Tameguri, T., 2009. Temporal change of characteristics of shallow volcano-tectonic earthquakes associated with increase in volcanic activity at Kuchinoerabujima Volcano, Japan. J. Volcanol. Geotherm. Res., 187, 1-12.

Yamamoto K., Ohkura, T., Yokoo, A., Tameguri, T., Sonoda, T., Inoue, H., 2017. Vertical ground deformation related with the 2014 and 2015 eruptions at Kuchierabujima Volcano, Japan detected by repeated precise leveling surveys, in this special issue.

H.YAKIWARA, S.HIRANO, Y.YAMASHITA, H.SHIMIZU, K.UCHIDA, K.UMAKOSHI, K.NAKAHIGASHI, H,MIYAMACHI, M.YAGI, H.KANEHARA, S.NAKAO